Journal of Crystal Growth 323 (2011) 84–87

Contents lists available at ScienceDirect

Journal of Crystal Growth

journal homepage: www.elsevier.com/locate/jcrysgro

Growth of cubic GaN on nano-patterned 3C-SiC/Si (0 0 1) substrates

R.M. Kemper *, M. Weinl, C. Mietze, M. Häberlen, T. Schupp, E. Tschumak, J.K.N. Lindner, K. Lischka, D.J. As

University of Paderborn, Department of Physics, Warburger Strasse 100, 33098 Paderborn, Germany

ARTICLE INFO

Available online 21 December 2010

Keywords:
A1. Crystal structure
A1. Defects
A1. Growth models
A1. Nanostructures
A3. Molecular beam epitaxy
B1. Nitrides

ABSTRACT

Non-polar relaxed cubic GaN was grown by molecular beam epitaxy (MBE) on nano-patterned 3C-SiC/Si (0 0 1) substrates with negligible hexagonal content and less defect density than in planar cubic GaN layers. Nano-patterning of 3C-SiC/Si (0 0 1) is achieved by self-ordered colloidal masks for the first time. The method presented here offers the possibility to create nano-patterned cubic GaN without the need for a GaN etching process and thus is a potential alternative to the conventional top–down fabrication techniques.

1. Introduction

Wide bandgap materials, especially group III-nitrides like GaN, are important for optoelectronic and electronic devices such as laser diodes and transistors [1–3]. Devices show best performance if fabricated on lattice-matched substrates since lattice-mismatch leads to the generation of misfit dislocations at the interface, which may reduce the performance of devices. Hence there is a commercial interest in nitride technologies to fabricate dislocation-free epilayers for high-quality GaN-based devices.

One method for elimination of misfit dislocations is the reduction of the growth area [4]. Defect reduction in mismatched systems was also demonstrated by the theory of nanoheteroepitaxy (NHE), which describes the selective growth on a nano-patterned (10–100 nm) substrate [5]. In contrast to planar heteroepitaxy NHE includes a distribution of the mismatch strain in the epilayer in three dimensions and a partitioning of strain between the epilayer and the substrate. NHE shows the possibility of growing dislocation-free epilayers on nonlattice matched nano-patterned substrates.

In hexagonal GaN inherent spontaneous and piezoelectric polarization fields are present along the *c*-axis because of the crystal symmetry [6]. Due to these fields, non-polar and semi-polar systems have attracted growing interest in the last few years [7]. One method to produce real non-polar materials is the growth of cubic GaN. There is a narrow window of experimental conditions to achieve heteroepitaxial growth of cubic GaN [8]. The most adequate substrate is 3C-SiC (0 0 1) with a misfit of 3.5%. The dislocation density of cubic GaN deposited on 3C-SiC (0 0 1) by plasma assisted molecular beam epitaxy (MBE) is $\sim 10^9$–10^{10} cm^{-2} [9]. A reduction in the dislocation density would lead to high performance devices. Best device performance would be reached by GaN layers grown on lattice-matched bulk GaN, but there is a shortage of low defect density bulk GaN substrates [10].

In this work, we demonstrate the growth of non-polar cubic GaN by molecular beam epitaxy (MBE) on nano-patterned 3C-SiC/Si (0 0 1) substrates with an extremely small content of the hexagonal phase. Nano-patterning of 3C-SiC/Si (0 0 1) is achieved with self-organized colloidal masks.

2. Experiment

The used substrates consist of 12 μm-thick 3C-SiC (0 0 1) films on top of 500 μm Si. 3C-SiC (0 0 1) was deposited by low-pressure chemical vapor deposition [11] and the surface was chemo-mechanically polished after growth process. The root mean square roughness is about 0.5–1 nm and the FWHM of the rocking curve is about 5 arcmin. To investigate GaN layers on nano-patterned substrates the 3C-SiC/Si (0 0 1) substrates were structured by nanosphere lithography (NSL). NSL is a low-cost method to produce regular nanoscale surface patterns of scalable size and a variety of motifs. Due to the hydrophobic character of SiC [12], the substrate was coated with ~16 nm of SiO_2 by plasma enhanced chemical vapor deposition followed by a cleaning process (H_2O:NH_3:H_2O_2=3:1:1). The surface was subsequently covered with a mask of 600 nm diameter polystyrene (PS) spheres, which are self-organized in a hexagonally closed packed monolayer [13]. This is achieved by the controlled drying of a droplet of an aqueous suspension of colloidal PS spheres. In a next step, the spheres were shrunken in oxygen plasma [14]. On top of the colloidal mask 60 nm of Ni was thermally evaporated and the PS spheres were removed. The Ni-mask coated 3C-SiC/Si (0 0 1) was etched vertically by 400 nm using reactive ion etching (10% O_2, 6.1% SF_6). After removing the metal using $FeCl_3$ and DI-water (1:3), the samples were

* Corresponding author. Tel.: +49 5251605848; fax: +49 5251605843.
E-mail address: rkemper@mail.uni-paderborn.de (R.M. Kemper).

0022-0248/$ - see front matter © 2010 Elsevier B.V. All rights reserved.
doi:10.1016/j.jcrysgro.2010.12.042

cleaned with a buffered oxide etching solution (NH_4F:H_2O:HF = 4:6:1). Altogether, this procedure allows the creation of surface patterns with a lateral feature size of some ten to a few hundred nanometers.

On these patterned 3C-SiC/Si (0 0 1) substrates 440 nm-thick cubic GaN (0 0 1) were grown by plasma assisted MBE. As a reference sample a 440 nm-thick cubic GaN epilayer was grown on an unstructured 3C-SiC/Si (0 0 1) for comparison. For both patterned and unpatterned substrates the growth temperature was 720 °C and a 1 ML Ga coverage at the surface was used to grow under optimum conditions [8]. Reflection high energy electron diffraction (RHEED) was used to monitor *in-situ* the crystalline nature of the sample surface. After growth the samples were characterized by atomic force microscopy (AFM), high-resolution X-ray diffraction (HRXRD), transmission electron microscopy (TEM) and room temperature micro photoluminescence (μ-PL).

3. Results and discussion

Fig. 1(a) shows the RHEED pattern ([1 1 0] azimuth) of a 440 nm-thick planar cubic GaN layer (reference sample). The long streaks indicate a two-dimensional surface. The reflections can be allocated to the cubic symmetry of the surface [15]. Fig. 1(b) illustrates the [1 1 0] azimuth RHEED pattern of the surface of a 440 nm-thick GaN layer grown on nano-structured 3C-SiC/Si (0 0 1). The RHEED pattern in Fig. 1(b) is similar to that of the planar cubic GaN layer. These RHEED patterns have been observed frequently during growth process (about every 50 nm). Together with the results of HRXRD (shown in Fig. 3) this clearly indicates the growth of cubic GaN on pre-patterned 3C-SiC/Si (0 0 1). Fig. 2(a) is a top view SEM image of the 440 nm cubic GaN on 3C-SiC/Si (0 0 1) nano-patterned by NSL. Fig. 2(b) shows an AFM image of the surface of selective-area-grown cubic GaN. Cubic GaN grows in islands with a width of 200–350 nm. The root mean square roughness on the surface of these islands varies from 1 to 3 nm. The strain and the lattice parameter of the selective-area-grown structures were investigated by HRXRD measurements at room temperature.

Fig. 3 displays an asymmetrical reciprocal space map around the (1 1 3) reflex of selectively grown cubic GaN.

Position 1 marks the literature value of 3C-SiC [16]. Position 2 presents the literature value [17] of planar cubic GaN and point 3 shows the experimental data of selectively grown cubic GaN. The selective-area-grown cubic GaN is relaxed to the 3C-SiC with a minimal residual tensile strain. The reason for the residual tensile strain can be found in different thermal expansion coefficients of cubic GaN and 3C-SiC [18]. The same measurements were done for the planar reference layer and show that there is equal strain in both cases. The lattice parameter in growth direction was determined to be 4.503 ± 0.001 Å. Additionally a negligible amount of hexagonal inclusions in the selective-area-grown cubic GaN is measured by (0 0 2) symmetrical reciprocal space maps (not shown). The FWHM of the rocking curve of selective-area-grown cubic GaN is about 29 arcmin and smaller than the FWHM of the rocking curve of the planar cubic GaN reference layer with 36 arcmin. Using the method of Gay et al. [9] the defect density of selective-area-grown cubic GaN is determined to be $4.5 \times 10^9/cm^2$ and $7.4 \times 10^9/cm^2$ for a planar layer.

In order to investigate the micro- and nano-structural features of the MBE grown GaN nanostructures, cross-sectional TEM samples were prepared by mechanical grinding and polishing followed by an ion beam thinning step. The samples were subsequently examined using a Philips CM200ST TEM operated at 200 kV.

Fig. 4 shows a TEM micrograph of the nano-structured sample taken along the [1 1 0] zone axis under a two-beam condition. It can clearly be observed that the 3C-SiC/Si (0 0 1) template was successfully structured yielding ~300 nm deep and roughly 400 nm wide trenches with a spacing of ~1.2 μm. MBE growth of GaN led to the deposition of about 400 nm high islands of cubic GaN epitaxially oriented with the 3C-SiC/Si (0 0 1) substrate as confirmed by selected area diffraction (SAD, not shown). The islands exhibit lateral facets that are inclined by ~10° with respect to the growth direction and additional facets on the top which are inclined by ~20° with respect to the sample template surface. Sanorpim et al. [15] have observed similar faceting of cubic GaN in their studies of epitaxial lateral overgrowth of (0 0 1)-oriented stripe-patterned GaAs with cubic GaN by MOVPE. The mechanism of facet formation is not completely understood yet and will be a topic of further studies.

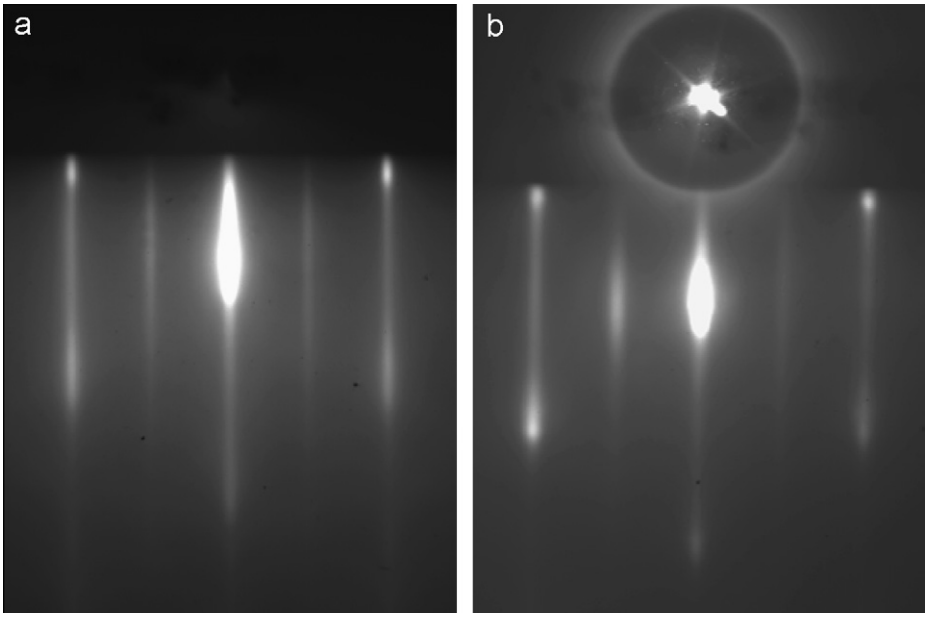

Fig. 1. (a) RHEED pattern of a 440 nm-thick cubic planar GaN on 3C-SiC/Si (0 0 1) and (b) RHEED pattern of a 440 nm-thick cubic GaN layer grown on nano-structured 3C-SiC/Si (0 0 1) (both images in [1 1 0] azimuth).

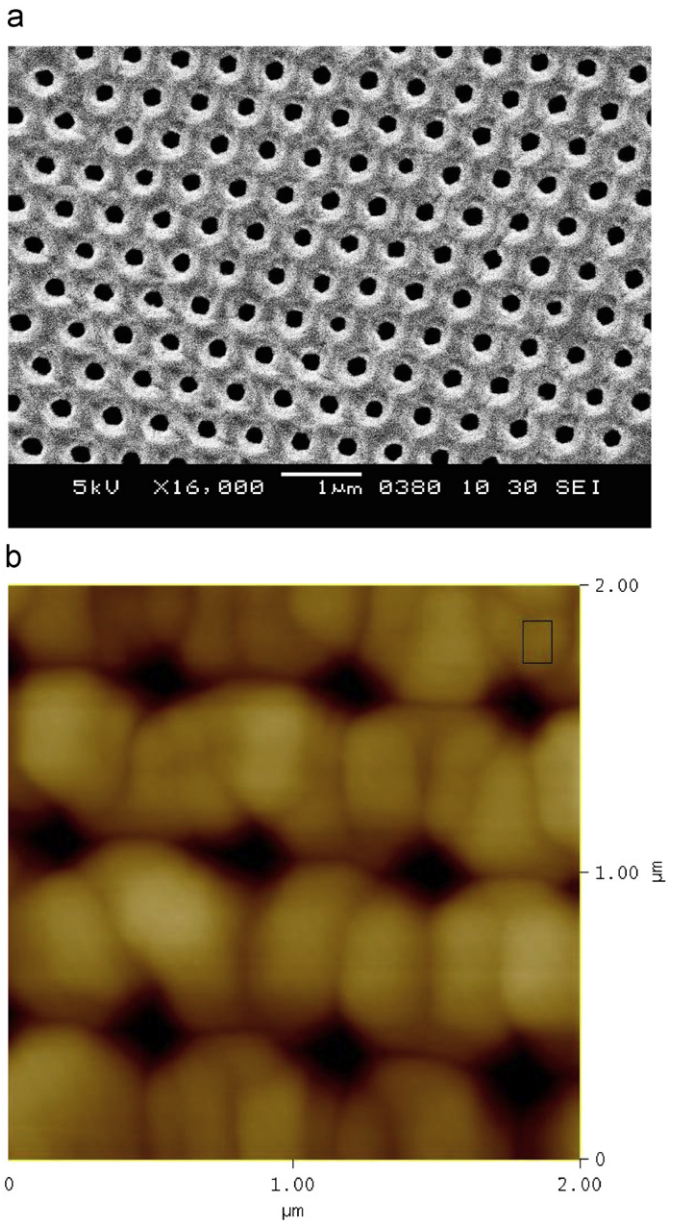

Fig. 2. (a) SEM image of 440 nm-thick cubic GaN on 3C-SiC/Si (0 0 1) nano-structured by NSL and (b) AFM image of 440 nm thick cubic GaN on 3C-SiC/Si (0 0 1).

The GaN islands shown in Fig. 4 contain stacking faults (SFs) mainly on the (1 1 1) planes, which appear as bright and dark linear contrast features and lead to streaks along the [1 1 1] direction in the [1 1 0] cubic GaN SAD pattern (Fig. 5(a)) taken from the middle island of Fig. 4. Additional streaks can be found along the [1 1 1] direction but they are significantly weaker indicating a much lower stacking fault density on these planes. This is consistent with observations in weak beam-dark-field images (not shown), which further support an asymmetric stacking fault density. This detail is also seen in the symmetrical (0 0 2) reciprocal space maps (not shown).

In addition to the reflections originating from cubic GaN and the stacking fault therein, weaker spots along the [1 1 1] direction can be found. All these additional reflections can be explained by the formation of a small fraction of hexagonal inclusions, which are predominantly formed along the [1 1 1] direction. Fig. 5(b) shows the expected positions of reflections in a SAD pattern originating from cubic GaN (filled circles) and from hexagonal inclusions (crosses) as simulated using JEMS v3.1410U2009 [19], assuming

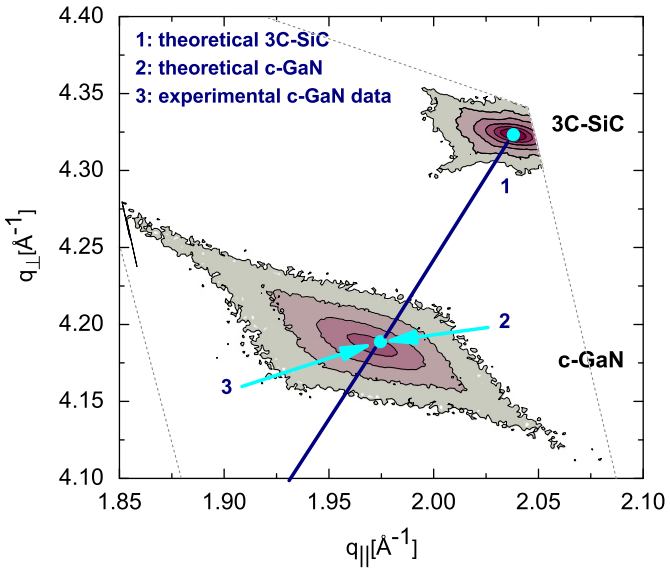

Fig. 3. Reciprocal Space Map around the (1 1 3) reflex of selective-area-grown cubic GaN.

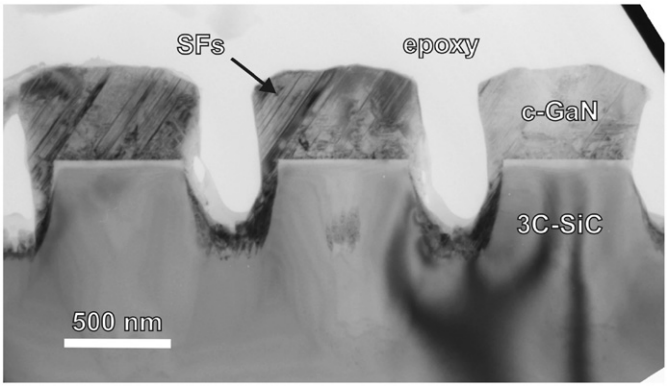

Fig. 4. Cross-sectional TEM image of the nano-structured cubic GaN sample taken along the [1 1 0] zone axis under a two-beam condition. Stacking faults along the [1 1 1] direction can be observed in the cubic GaN and are marked with 'SFs'.

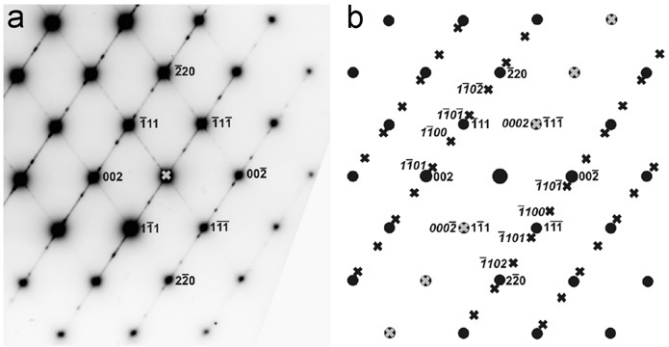

Fig. 5. (a): Selected area diffraction (SAD) pattern taken from the middle cubic GaN island in Fig. 4 along the [1 1 0] cubic GaN zone axis with the main reflections indexed. Streaks along the [1 1 1] and [1 1 1] indicate the formation of stacking faults along these directions. (b) Simulated SAD pattern of cubic GaN along the [1 1 0] direction (filled circles) together with the simulation of h-GaN viewed along the [1 1 2 0] direction (crossed). The good match of the experimental pattern (a) with the simulation (b) indicates the presence of a small fraction of hexagonal inclusions along the [1 1 1] direction within the cubic GaN islands.

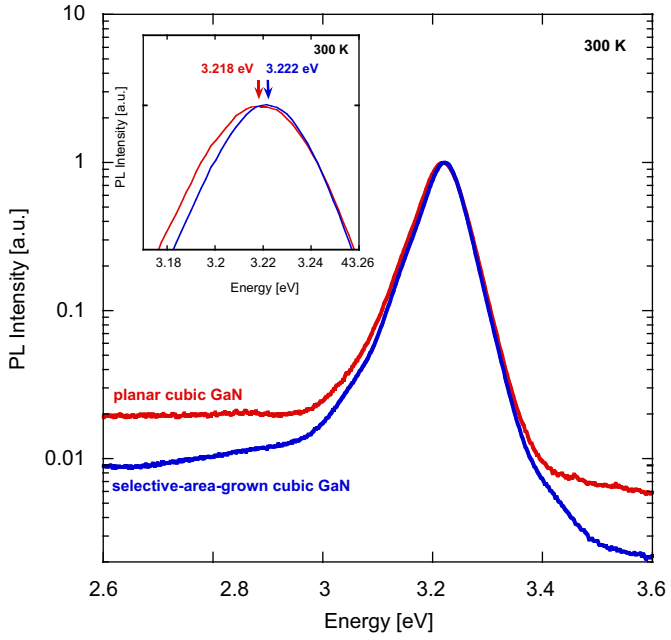

Fig. 6. Room temperature μ-PL spectra of a planar cubic GaN epilayer (red) and selective-area-grown cubic GaN (blue). (For interpretation of the references to color in this figure legend, the reader is referred to the web version of this article.)

an epitaxial relationship of [0 0 0 2]h-GaN || [1̲ 1 1̲]c-GaN and [1 1 0]c-GaN || [1 1 2̲ 0]h-GaN. The absence of similar diffraction spots along the [1̲ 1 1] direction indicates a negligible amount of hexagonal inclusions along this direction, in perfect agreement to a much smaller density of stacking faults on the (1̲ 1 1) plane. This points to a relation between the stacking faults and the hexagonal inclusions.

The optical properties of the patterned cubic GaN layer were studied by room temperature μ-PL measurements. Luminescence was excited by the 325 nm line of a He–Cd laser with a power of 400 μW on the sample surface (beam diameter 1–2 μm). In Fig. 6 the spectra of cubic GaN planar reference layer sample (red curve) and selective-area-grown cubic GaN sample (blue curve) are depicted. The spectra show that there are no luminescence bands of the hexagonal phase, which is a further indication that our nano-patterned GaN has negligible small hexagonal inclusions.

The peak of the band-edge luminescence of the reference layer is at 3.218 eV. This value agrees well with the literature value of 3.21 eV for cubic GaN grown on GaAs [20]. There is a blue shift of 4 meV in the band-edge transition (3.222 eV) of the selective-area-grown cubic GaN sample. The shift to a higher bandgap energy indicates that the tensile strain in the selective-area-grown cubic GaN that was shown by HRXRD is lower than that in the planar cubic GaN layer.

4. Conclusion

The growth of non-polar cubic GaN via rf-plasma assisted MBE under Ga-rich growth conditions on pre-structured 3C-SiC/Si (0 0 1) is demonstrated. Nano-patterning of 3C-SiC/Si (0 0 1) substrate was realized by nanosphere lithography. The evidence that the selective-area-grown GaN crystallizes in the zincblende structure is given by several independent characterization methods. AFM measurements show that cubic GaN grows in small islands with a diameter of 200–350 nm. The root mean square roughness on the surface of these islands varies from 1–3 nm. HRXRD measurements exhibit that selective-area-grown cubic GaN as well as planar epilayers are relaxed on 3C-SiC/Si (0 0 1) with minimal residual tensile strain. The selective-area-grown cubic GaN exhibits lateral facets that are evidenced by cross-sectional TEM measurements. The GaN islands show stacking faults and a small fraction of hexagonal inclusions. μ-PL measurements at room temperature demonstrate that the selective-area-grown cubic GaN is less tensile strained than a planar reference layer. However, to draw a conclusion about the GaN islands regarding to the theory of nanoheteroepitaxy the size of the islands has to be scaled down. Work in this area is under way.

Acknowledgements

The authors would like to thank W. Reiber and B. Knoblich (University of Augsburg) for assistance with the TEM specimen preparation as well as Prof. Dr.- Ing. H.-J. Meier (University of Paderborn) and especially Dipl.-Ing. K. Duschik for access to the TEM. The work at Paderborn was financially supported by the German Science Foundation (DFG).

References

[1] S. Nakamura, I. Mukai, M. Senok, Appl. Phys. Lett. 64 (1994) 1687.
[2] S. Rajan, P. Waltereit, C. Poblenz, S.J. Heikman, D.S. Green, J.S. Speck, U.K. Mishra, IEEE Electron. Device Lett. 25 (2004) 247.
[3] E. Tschumak, R. Granzer, J.K.N. Lindner, F. Schweiz, K. Lischka, H. Nagasawa, M. Abe, D.J. As, Appl. Phys. Lett. 96 (2010) 253501.
[4] E.A. Fitzgerald, G.P. Watson, R.E. Proano, D.G. Ast, J. Appl. Phys. 65 (1989) 2220.
[5] D. Zubia, S.D. Hersee, J. Appl. Phys. 85 (1999) 6492.
[6] F. Bernardini, V. Fiorentini, D. Vanderbilt, Phys. Rev. B 56 (1997) R10024.
[7] P. Waltereit, O. Brandt, A. Trampert, H.T. Grahn, J. Menninger, M. Reiche, K.H. Ploog, Nature 406 (2000) 865.
[8] J. Schörmann, S. Potthast, D.J. As, K. Lischka, Appl. Phys. Lett. 90 (2009) 041918.
[9] P. Gay, P.B. Hirsch, A. Kelly, Acta Metall. 1 (1953) 315.
[10] S.V. Novikov, N.M. Stanton, R.P. Campion, C.T. Foxon, A.J. Kent, J. Cryst. Growth 310 (2008) 3964.
[11] T. Chassagne, A. Leycuras, C. Balloud, P. Arcade, H. Peyre, S. Juillaguet, Mater. Sci. Forum 457-460 (2004) 273–276.
[12] G. Cicero, G. Galli, J. Phys. Chem. B 108 (2004) 16518.
[13] J.K.N. Lindner, C. Seider, F. Fischer, M. Weinl, B. Stritzker, Nucl. Instrum. Methods Phys. Res. B 267 (2009) 1394.
[14] D. Gogel, M. Weinl, J.K.N. Lindner, B. Stritzker, J. Optoelectron. Adv. Mat. 12 (3) (2010) 740–744.
[15] S. Sanorpim, E. Takuma, H. Ichinose, R. Katayama, K. Onabe, Phys. Status Solidi (b) 244 (6) (2007) 1769.
[16] A. Taylor, R.M. Jones, in: J.R. O'Connor, J. Smiltens (Eds.), Silicon Carbide-A High Temperature Semiconductor, Pergamon Press, 1960, p. 147.
[17] S. Strite, J. Juan, Z. Li, A. Salvador, H. Chen, D.J. Smith, W.J. Choyke, H. Morkoc, J. Vac. Sci. Technol. B 9 (4) (1991) 1924.
[18] J. Wu, H. Yaguchi, B.P. Zhang, Y. Segawa, K. Onabe, Y. Shiraki, Phys. Status Solidi (a) 180 (2000) 403.
[19] P.A. Stadelmann, Ultramicroscopy 21 (2) (1987) 131.
[20] D.J. As, F. Schmilgus, C. Wang, B. Schöttker, D. Schikora, K. Lischka, Appl. Phys. Lett. 70 (1997) 1311.